ACS Macro Letters

Letter

pubs.acs.org/macroletters

Macroscopic and Microscopic Elasticity of Heterogeneous Polymer Gels

Fany Di Lorenzo,[†,‡,§] Johannes Hellwig,[†,∥] Regine von Klitzing,[∥] and Sebastian Seiffert*[,‡,§,⊥]

[‡]Helmholtz-Zentrum Berlin, Soft Matter and Functional Materials, Hahn-Meitner-Platz 1, D-14109 Berlin, Germany

[§]Helmholtz Virtual Institute "Multifunctional Biomaterials for Medicine", Kantstr. 55, D-14513 Teltow, Germany

[∥]Technische Universität Berlin, Stranski-Laboratorium, Strasse des 17. Juni 124, D-10623 Berlin, Germany

[⊥]Freie Universität Berlin, Institute of Chemistry and Biochemistry, Takustr. 3, D-14195 Berlin, Germany

Supporting Information

ABSTRACT: Polymer-network gels often exhibit local defects and spatial heterogeneity of their cross-linking density, which may differently affect their elasticity on microscopic and macroscopic scales. To appraise this effect, we prepare polymeric gels with defined extents of nanostructural heterogeneity and use atomic force microscopy to probe their local microscopic Young's moduli in comparison to their macroscopic elastic moduli measured by shear rheology. In this comparison, the moduli of the heterogeneous gels are found to be progressively smaller if the length scale of the probed gel region exceeds the size of the purposely imparted polymer-network heterogeneities. This finding can be explained with a conceptual picture of nonaffine deformation of the densely cross-linked polymer network domains in the heterogeneous gels.

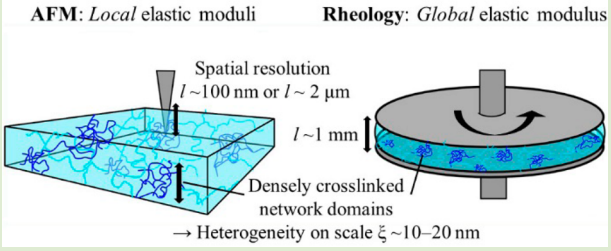

Polymer gels consist of three-dimensional assemblies of cross-linked polymer chains swollen in a solvent.[1,2] If they are formed by uncontrolled polymerization, these gels exhibit an inhomogeneous spacing of their network cross-linking junctions in the form of densely cross-linked local domains randomly distributed within a loosely cross-linked background.[3−6] As a result, such heterogeneous polymer gels display pronounced concentration fluctuations on length scales of several ten nanometers[7] that have been investigated by light, X-ray, neutron scattering,[8−11] NMR spectroscopy,[12,13] and microscopy techniques.[14,15] It has been shown that the elastic modulus of a gel, as probed by rheology, decreases with increasing degree of inhomogeneity in the gel, as probed by light scattering,[6,16,17] such that the elastic moduli of heterogeneous gels synthesized by free radical copolymerization of mono- and bifunctional monomers[6,16,18] are lower than the moduli of more homogeneous gels prepared by either controlled polymerization or by postpolymerization cross-linking of linear precursor chains.[19−21] Nevertheless, the elastic moduli of both of these types of gels are generally lower than what would be expected from their content of cross-linker on the basis of the statistical theory of rubber elasticity.[22,23] These observations have been explained by two different arguments. One argument is the formation of elastically ineffective network defects such as loops and dangling chains during the gel-network polymerization.[24] The other argument is the possible presence of very short network strands with a length close to the persistence length of the polymer, which are too rigid to deform and store elastic energy. In densely cross-linked domains that contain multiple of such short chains, several cross-links therefore just act as one single cross-linking supernode of high functionality but limited ability for elastic-energy storage.[25,26] In an extension of this conceptual picture, it was suggested that heterogeneous gels deform in a nonaffine fashion.[27−29] One hypothesis is that stiff, densely cross-linked gel domains deform less than the surrounding soft, loosely cross-linked background and, therefore, just partially contribute to elastic-energy storage.[30]

To challenge the hypothesis of nonaffine deformation and to clarify whether and to which extent each of the above aspects is responsible for the low elastic moduli of heterogeneous polymer gels, we probe poly(*N*-isopropylacrylamide) (pNIPAm) gels with well-defined extents of polymer-cross-linking heterogeneity. We prepare these gels by controlled cross-linking of prepolymerized linear chains containing a determined low amount of photo-cross-linkable moieties, mixed in different ratios with prepolymerized linear chains containing a high amount of photo-cross-linkable moieties. With this approach, we obtain heterogeneous polymer gels whose distribution of network-strand lengths is predetermined by the spacing between the cross-linkable moieties in the precursor chains. To discern between the effects of topological network defects and nonaffine deformation on the gel elasticity, we probe these gels on different experimental length scales. For this purpose, we use atomic force microscopy to measure the local

Received: April 1, 2015
Accepted: June 17, 2015
Published: June 18, 2015

DOI: 10.1021/acsmacrolett.5b00228
ACS Macro Lett. 2015, 4, 698−703

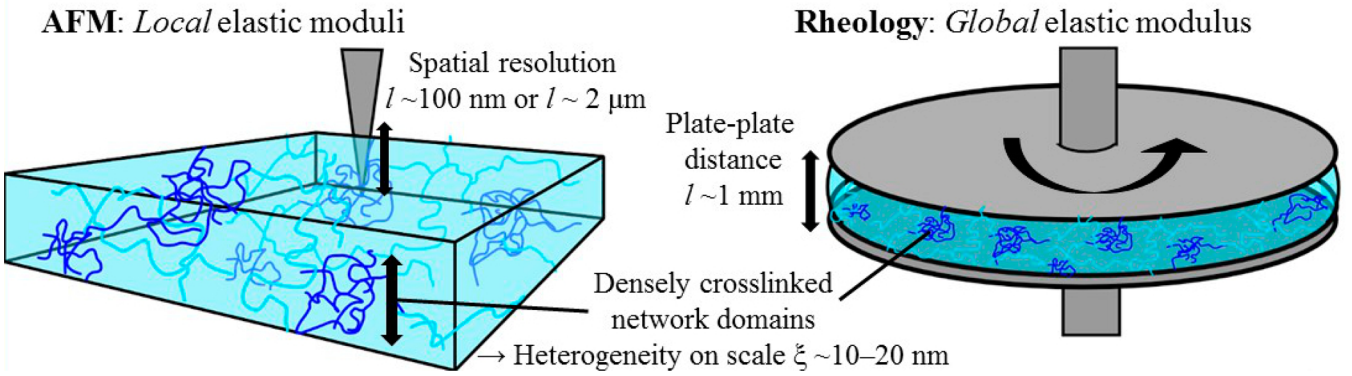

Figure 1. Concept of this work: we use atomic force microscopy (AFM) to measure the local Young's moduli of polymer gels with determined inhomogeneous polymer-network cross-linking density on a length scale of $\xi \sim 10-20$ nm, probing them with a spatial resolution that is either of the order of the size of this inhomogeneity ($l \sim 100$ nm $\sim 5\xi$) or larger ($l \sim 2$ μm $\sim 100\xi$) (left). We also measure the global macroscopic moduli of the same gels by oscillatory shear rheology on an experimental length scale of several mm ($l > 10^6\xi$) (right). Comparison of these micro- and macroscopic moduli serves to discern the contributions of topological connectivity defects and potentially nonaffine deformation of nanoscopic local dense regions in the gel polymer networks.

microscopic Young's moduli of gel regions on a length scale close to that of the nanostructural inhomogeneities within the gels ($\xi \sim 10-20$ nm), as shown in Figure 1 (left). These experiments mostly probe the effect of topological network defects on the elasticity of the different gel regions. In addition, we compare these local microscopic moduli with the global macroscopic shear moduli of the same polymer gels measured by shear rheology in the linear viscoelastic regime at a strain of $\gamma = 1\%$.[17] These macroscopic moduli are measured on mm-sized gel samples that are much larger than the length scale of their internal structural inhomogeneities, as shown in Figure 1 (right). These experiments therefore probe both the effect of topological network defects and that of a potentially nonaffine deformation of densely cross-linked local domains.

We prepare heterogeneous gels by photo-cross-linking minor fractions (8 or 27 wt %) of linear pNIPAm chains containing a high amount (3.15 mol % of the monomer repeat units) of photo-cross-linkable dimethylmaleimide (DMMI) moieties, mixed in solution with major fractions (92 or 73 wt %) of linear pNIPAm chains containing a low amount (0.7 mol % of the monomer repeat units) of DMMI moieties. In addition, we prepare better homogeneous gels that contain the same average amount of photo-cross-linkable moieties as the heterogeneous gels, but this time obtained by photo-cross-linking of statistically all-identical linear chains, all functionalized with either 0.9 mol % (sample *Homo*-0.9) or 1.35 mol % (sample *Homo*-1.3) of DMMI moieties. Upon UV irradiation of the polymer solutions in the presence of a photosensitizer, sodium thioxanthone-2,7-disulfonate, the DMMI moieties dimerize, leading to polymer-network formation and to gelation of the polymer solutions.[19,31] In the samples *Homo*-0.9 and *Homo*-1.3, the photo-cross-linkable moieties are randomly distributed among statistically all-identical polymer chains; by contrast, in the heterogeneous gels that contain the same overall amounts of DMMI, *Hetero*-0.9 and *Hetero*-1.3, the photo-cross-linkable moieties are purposely inhomogeneously distributed between the different fractions of precursor polymer chains. This creates gels with spatially varying cross-linking densities on length scales of $\xi \sim 10-20$ nm, as determined by the radii of the differently prefunctionalized precursor chains and as confirmed by static light scattering.[17]

The Young's moduli of these polymer gels are determined by force measurements with an MFP3D-Bio AFM (Asylums Research) at three different areas on each polymer gel, each probed by recording a force map with 90×90 μm^2 area after the gels are swollen in water. Each force map consists of 100 force curves, giving 300 force curves in total for each polymer gel. To determine the Young's moduli of the polymer gels on two different length scales, we probe them using either a tip with radius $R = 30$ nm and an indentation depth of $l \sim 100$ nm or a spherical probe with radius $R = 3.35$ μm and an indentation depth of ~300 nm. For the measurements with the tip, the experimental length scale is $l \sim 100$ nm, whereas for the measurements with the sphere, the experimental length scale is $l \sim 2$ μm.

The average Young's moduli of the homogeneous and heterogeneous polymer gels measured by AFM on a length scale of $l \sim 100$ nm are $E_{\text{Homo-0.9,AFM}} = (6.2 \pm 1.0)$ kPa for the homogeneous gel containing 0.9 mol % of DMMI, $E_{\text{Hetero-0.9,AFM}} = (4.2 \pm 1.2)$ kPa for the corresponding heterogeneous gel, $E_{\text{Homo-1.3,AFM}} = (15.4 \pm 1.7)$ kPa for the homogeneous gel containing 1.35 mol % of DMMI, and $E_{\text{Hetero-1.3,AFM}} = (11.8 \pm 2.2)$ kPa for the corresponding heterogeneous gel, as shown in Figure 2A and listed in Table 1. As expected, the mean Young's moduli of the heterogeneous polymer gels are lower than those of the corresponding homogeneous gels. In addition, the distribution of the moduli measured on a length scale of $l \sim 100$ nm is wider for the heterogeneous gels than for the homogeneous gels, and their relative standard deviation, RSD, is about two times larger for the heterogeneous gels (RSD = 19–28%) than for the homogeneous gels (RSD = 11–16%) as is also shown in Figure 2; this indicates the presence of larger fluctuations of the polymer segmental concentration and of the cross-linking density. By contrast, the distributions of the Young's moduli measured by AFM on an experimental length scale of $l \sim 2$ μm are less broad, and their relative standard deviations are approximately the same for all homogeneous and heterogeneous gel samples investigated (RSD = 3.5–3.9%), as shown in Figure 2B and listed in Table 1. This can be explained by considering that the experimental length scale of these measurements, $l \sim 2$ μm, is ~100× larger than the length scale of the gel cross-linking inhomogeneities, $\xi \sim 10-20$ nm and, therefore, the measured Young's moduli average over many different local structural domains.

We also measure the Young's moduli of two homogeneous gels obtained by photo-cross-linking the polymer chains used to

DOI: 10.1021/acsmacrolett.5b00228
ACS Macro Lett. 2015, 4, 698–703

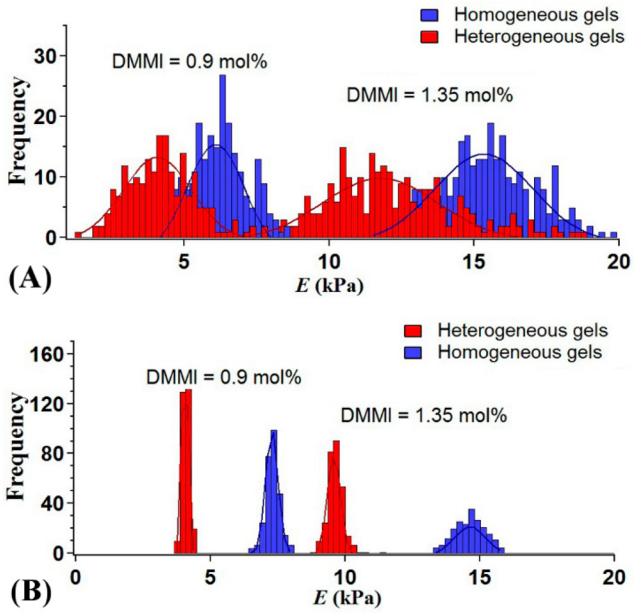

Figure 2. Distributions of Young's moduli of the two homogeneous gels (*blue*) and of the two corresponding heterogeneous gels (*red*) investigated in this work, measured on 300 different local gel regions on an experimental length scale of $l \sim 100$ nm (A) and $l \sim 2$ μm (B). The two distributions on the left refer to the gels *Homo*-0.9 and *Hetero*-0.9, whereas the two moduli distributions on the right refer to the gels *Homo*-1.3 and *Hetero*-1.3.

Table 1. Young's Moduli, E, and Crosslinking Efficiency, ν_{eff}/ν, of Homo- and Heterogeneous pNIPAm Hydrogel Samples Measured by AFM and Rheology on Different Experimental Length Scales, l[a]

sample	E_{AFM} (kPa); $l \sim 100$ nm	E_{AFM} (kPa); $l \sim 2$ μm	E_{Rheo} (kPa); $l > 1$ mm
Homo-0.9	6.2 ± 1.0	7.3 ± 0.3	6.6
Hetero-0.9	4.2 ± 1.2	4.1 ± 0.2	4.4
Homo-1.3	15.4 ± 1.7	14.6 ± 0.5	13.3
Hetero-1.3	11.8 ± 2.2	9.6 ± 0.3	5.7
sample	$(\nu_{eff}/\nu)_{AFM}$ (%); $l \sim 100$ nm	$(\nu_{eff}/\nu)_{AFM}$ (%); $l \sim 2$ μm	$(\nu_{eff}/\nu)_{Rheo}$ (%); $l > 1$ mm
Homo-0.9	27 ± 5	31 ± 1.3	26
Hetero-0.9	25 ± 7	23 ± 0.9	17
Homo-1.3	40 ± 4	38 ± 0.8	35
Hetero-1.3	38 ± 6	31 ± 1.1	15

[a] E_{AFM}: Young's modulus measured by rheology on a length scale of $l \sim 100$ nm or $l \sim 2$ μm; E_{Rheo}: Young's modulus inferred from the shear elastic modulus measured by rheology on a length scale of several millimeters ($l > 1$ mm); $(\nu_{eff}/\nu)_{AFM}$: cross-linking efficiency calculated from the Young's modulus measured by AFM and corrected by consideration of different extents of gel swelling; $(\nu_{eff}/\nu)_{Rheo}$: cross-linking efficiency calculated from the Young's modulus inferred from the shear elastic modulus measured by rheology on the gels at their preparation state without additional swelling.

form the heterogeneous samples above, but this time without mixing them. These homogeneous gels contain either 0.7 or 3.15 mol % of DMMI moieties randomly distributed between the polymer chains, and their average microscopic Young's moduli measured on a length scale of $l \sim 100$ nm are $E_{Homo\text{-}0.7,AFM} = (3.6 \pm 0.9)$ kPa and $E_{Homo\text{-}3.15,AFM} = (50.9 \pm 4.3)$ kPa. Furthermore, we infer the macroscopic Young's moduli of the gels from their shear moduli, G', measured by shear rheology in the gel-preparation state,[17] as $E_{Rheo} = 2\,G'(1 + p)$,[32] where $p \approx 0.33$ is the Poisson ratio of pNIPAm gels.[33,34] We find that, for all our homogeneous gels, the average microscopic Young's moduli measured by AFM, E_{AFM}, and the global macroscopic Young's moduli derived from rheology, E_{Rheo}, are approximately equal, as shown in Figure 3A and listed in Table 1. By contrast, for the heterogeneous gel containing the largest amount of densely cross-linked chains, *Hetero*-1.3, the average microscopic Young's modulus, $E_{Hetero\text{-}1.3,AFM}$, is about 2× larger than the macroscopic Young's modulus, $E_{Hetero\text{-}1.3,Rheo}$, as also shown in Figure 3A and listed in Table 1.

To explain these results, we consider the efficiency of cross-linking defined as ν_{eff}/ν, where ν is the ideally achievable concentration of network strands calculated from the concentration of DMMI moieties in the gels as $\nu = c_{DMMI}$, whereas ν_{eff} is the actual concentration of elastically active chains, inferred from the shear elastic moduli of the gels, $G' = (\nu_{eff}/2)kT$, according to the statistical theory of rubber elasticity for a phantom network with tetrafunctional cross-links.[22,23] In this estimation, G' is either directly measured by shear rheology or calculated from the Young's modulus measured by AFM as $G' = E_{AFM}/(2(1 + p))$. For a defect-free ideal network where every two DMMI moieties are converted to a cross-link and all network strands thus formed contribute equally to elasticity, $\nu_{eff}/\nu = 100\%$, whereas this value decreases if the fraction of elastically ineffective network strands increases. From the AFM measurements, it results that the cross-linking efficiency of the homogeneous gels investigated in this work is 20−60% and that it increases with increasing content of DMMI moieties in the precursor polymers, as shown in Figure 3B. This result indicates that the polymer gels of this work differ strongly from gels obtained by free radical copolymerization of monomers, whose cross-linking efficiency usually decreases with increasing concentration of cross-linker.[16,18] This is because, in gels synthesized from monomers, high concentrations of cross-linkers lead to formation of very short network strands and cross-linking supernodes. By contrast, in the gels of this work, the length of the network strands is predetermined by the spacing between the DMMI moieties in the precursor chains, which is at least 3× larger than the persistence length of pNIPAm.[35] Thus, the cross-linking efficiency increases with the probability that each DMMI moiety finds another one in its proximity during the photogelation, thereby increasing with the fraction of DMMI moieties in the precursor polymer chains. This observation also indicates that the formation of elastically inactive loops, whose probability also increases with increasing fraction of DMMI moieties, does not significantly affect the elasticity of the gels obtained. This is because the precursor polymer chains are cross-linked in solutions at a concentration at which the chains strongly overlap, and therefore, the probability of intermolecular cross-linking is higher than that of intramolecular cross-linking. By contrast, if loops had a relevant impact on the elasticity of gels obtained by cross-linking linear chains, the cross-linking efficiency would be lower at a higher concentration of cross-linkable moieties.

We can also appraise the amount of dangling chains in our gels by knowledge of the molecular weight of the precursor chains from which they were synthesized, determined by size

DOI: 10.1021/acsmacrolett.5b00228
ACS Macro Lett. 2015, 4, 698−703

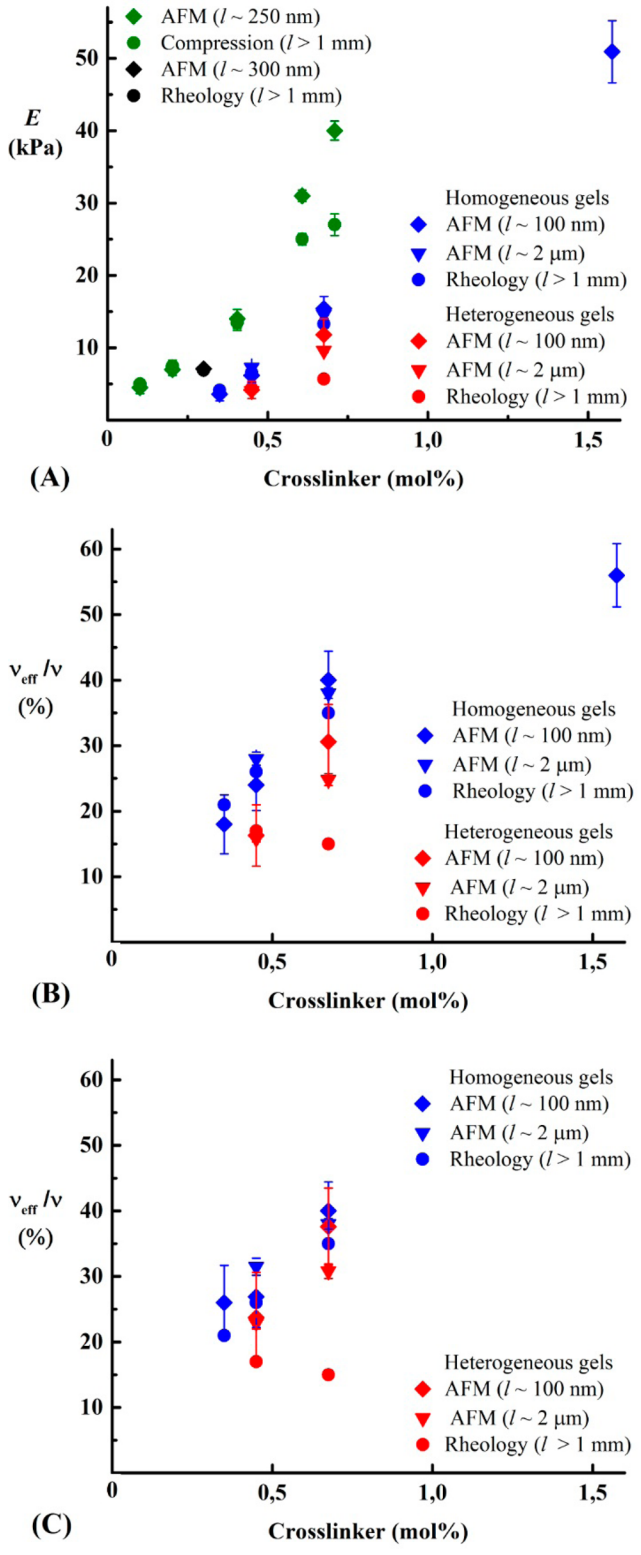

Figure 3. Young's moduli (A) and cross-linking efficiencies (concentration of elastically effective network chains, ν_{eff}, relative to the theoretically possible concentration of network strands, ν; B, C) of different types of polymer gels as a function of the content of cross-linker. (B) Cross-linking efficiency estimated without accounting for the gel swelling; by contrast, in (C), the cross-linking efficiency is recalculated after estimation of the extent of swelling of the gels. Blue symbols are used to denote the homogeneous pNIPAm gels investigated in this work, whereas red symbols refer to the heterogeneous pNIPAm gels of this work. In addition, green symbols represent data measured on PVP gels in ref 36, and black symbols refer to data recorded on pAAm gels from ref 37. Diamonds denote the *average* local microscopic moduli measured by AFM on experimental length scales of $l \sim 100-300$ nm; the error bars represent the standard deviation of the distribution of these Young's moduli, which is much larger than the experimental uncertainty. Triangles refer to the *average* local microscopic moduli measured by AFM on an experimental length scale of $l \sim 2$ μm. Circles denote the *global* macroscopic Young's moduli inferred from either shear rheology or compression measurements on a length scale of several millimeters, $l > 1$ mm.

exclusion chromatography,[17] and by knowledge of their content of DMMI, determined by UV–vis absorption photometry.[17] As the precursor chains do not carry DMMI groups right on their chain termini, each precursor polymer chain will intrinsically create two dangling chain ends in the cross-linked polymer network. The amount of these intrinsic dangling chains relative to the total amount of network strands of the polymer network is $D = n_{\text{dangling chains}}/n_{\text{total chains}} = 2/(n_{\text{DMMI}} + 1)$, where n_{DMMI} is the average number of DMMI moieties in the precursor polymer chains. We find that $D \approx 7\%$ for the sample *Homo*-0.9, $D \approx 9\%$ for the sample *Hetero*-0.9, $D \approx 4\%$ for the sample *Homo*-2, and $D \approx 8\%$ for the corresponding heterogeneous gel. This indicates that the loss in elastically active chains due to dangling chains is <10% for all samples investigated.

The cross-linking efficiency of the heterogeneous gels is markedly lower than that of the corresponding homogeneous gels, as shown in Figure 3B; this cannot be explained solely by the slightly larger ($\pm$2–4%) amounts of dangling chains in them. In addition, the cross-linking efficiency calculated from the macroscopic elastic moduli measured by rheology, $(\nu_{\text{eff}}/\nu)_{\text{Rheo}}$, decreases with increasing the concentration of cross-linkable DMMI groups and thus the extent of heterogeneity of the gel, as shown in Figure 3B and listed in Table 1. By contrast, the cross-linking efficiency calculated from the average Young's moduli measured by AFM on the heterogeneous gels, $(\nu_{\text{eff}}/\nu)_{\text{AFM}}$, increases with the concentration of cross-linkable DMMI groups, as also shown in Figure 3B.

An additional factor to be considered in our analysis is the volume fraction of the gels. This volume fraction is $\phi_0 = 0.09$ in the gel preparation state and during the macroscopic rheology measurements. By contrast, the AFM measurements are carried out after the gels are further swollen in water, the extent of which depends on their effective cross-linking densities at preparation. We estimate the volume fraction of the gels after swelling, φ, by use of the Flory–Rehner theory,[22,38–40] as detailed in the Supporting Information. We find that upon swelling, the volume fraction of the sample *Homo*-0.9 decreases from $\phi_0 = 0.090$ to $\varphi_{Homo\text{-}0.9} \approx 0.082$, whereas $\varphi_{Hetero\text{-}0.9} \approx 0.068$ for the corresponding heterogeneous gel *Hetero*-0.9, and $\varphi_{Hetero\text{-}1.3} \approx 0.077$ for the sample *Hetero*-1.3. In addition, we estimate that the gel with the highest effective cross-linking density, *Hetero*-1.3, does not swell after addition of water. With these estimations, we recalculate ν_{eff}/ν from the Young's moduli measured by AFM on the swollen gels, considering that the volume fraction of the heterogeneous gels is lower than that of the corresponding homogeneous gels, because of their more pronounced swelling. We find that these recalculated cross-linking efficiencies are only slightly lower for the heterogeneous gels than for the homogeneous gels, as shown in Figure 3C and listed in Table 1. This finding means that the observation that

DOI: 10.1021/acsmacrolett.5b00228
ACS Macro Lett. 2015, 4, 698–703

the Young's moduli of the heterogeneous gels measured by AFM are smaller than those of the heterogeneous gels is mostly due to their more pronounced swelling. As a result, if the ideally achievable density of elastic chains in the gels is estimated by considering the different extent of swelling of the gels, the cross-linking efficiency measured by AFM is similar for both homogeneous and heterogeneous samples.

In addition, the fact that the cross-linking efficiency calculated from the average microscopic moduli measured by AFM is much larger than the cross-linking efficiency calculated from the macroscopic moduli measured by rheology, both of them listed in Table 1, supports the hypothesis of nonaffine deformation of the different network domains.[30] The heterogeneous samples contain a significant amount of densely cross-linked network domains; if these gels are probed on a length scale similar to that of these domains ($\xi \sim 10-20$ nm), the cross-linking efficiency calculated from the Young's moduli averaged from different gel regions should be equal to the cross-linking efficiency of a homogeneous gel with the same average cross-linking density; but if the same gels are probed on a slightly larger length scale ($l \sim 100$ nm, corresponding to $\sim 5\xi$), as in our AFM measurements, the obtained average microscopic elastic moduli are slightly smaller than that of corresponding homogeneous gels. In notable contrast, if the gels are probed on a larger length scale ($l \sim 2$ μm, corresponding to $\sim 100\xi$), or even on a macroscopic length scale ($l > 1$ mm, corresponding to more than $10^6\xi$), as in our rheology experiments, the measured cross-linking efficiency is much lower, because the densely cross-linked regions are embedded in a soft, loosely cross-linked background and remain mostly undeformed and, therefore, contribute only to a limited extent to elastic energy storage. In addition, the width of the distributions of the measured Young's moduli decreases as the experimental length scale departs from the size of the gel nanostructural inhomogeneities and as the experiments average over gel regions larger than the densely cross-linked network domains. This effect is more pronounced for the sample *Hetero*-1.3 than for the sample *Hetero*-0.9, because the gel *Hetero*-1.3 contains a larger amount of highly DMMI-functionalized polymer chains (27 wt % compared to 8 wt %).

Finally, we compare our analyses to experimental data collected in other studies, where the Young's moduli of cross-linked poly(vinylpiridine) (PVP)[36] and poly(acrylamide) (PAAm)[37] gels were measured both on a microscopic scale by AFM and on a macroscopic scale by either shear rheology or by compression measurements. These gels were prepared by free-radically initiated polymerization of monomers and cross-linkers at different concentrations. For the gel samples prepared at low concentrations of cross-linker, therefore, exhibiting a more homogeneous nanostructure, the measured Young's moduli are not dependent on the microscopic or macroscopic length scale of observation, as shown in Figure 3A.[36,37] By contrast, if the concentration of cross-linker during the gel synthesis is higher than a certain threshold, the gels are heterogeneous, and their Young's moduli measured by AFM on a length scale of ~250 nm are much larger than the moduli measured by compression of the gel on a length scale of several mm,[36] as also shown in Figure 3A.

The experiments of this work do not allow us to completely disentangle the effects of topological defects and nonaffine deformation on the elasticity of heterogeneous gels, because the length scale of observation is always larger than the length scale of structural inhomogeneity. However, when we probe our gels by AFM on a length scale of ~100 nm, we investigate the effect of topological defects on the gel elasticity, while the effect of nonaffine deformation of the different network domains is small, because the elasticity is averaged over only ~5 network domains with sizes determined by the precursor polymer radii and estimated by static light scattering.[17] By contrast, when we increase the length scale of observation, as we do in rheology measurements, the effect of topological defects on the gel elasticity should be the same as in the AFM measurements, but the effect of nonaffine deformation is much larger, as we simultaneously probe $\sim 10^6$ different network domains.

This work clarifies and quantifies the different contributions of nanostructural complexity to the low elastic moduli of heterogeneous gels. It shows that the elasticity of gels with heterogeneous nanostructure depends on both the type and on the size of network heterogeneities compared to the length scale of the gel region probed. The effect of heterogeneity on the elastic moduli of gels is quantified by the cross-linking efficiency, which is 100% for ideally homogeneous gels and decreases with increasing heterogeneity. In gels prepared by cross-linking of linear prepolymerized chains, the cross-linking efficiency increases with the concentration of cross-linkable moieties in the precursor chains, in contrast to what has been observed for gels prepared by uncontrolled cross-linking copolymerization of monomers.[16,18] In addition, in gels made by cross-linking of linear precursor chains, the effect of loops on the elasticity is not significant if the gel formation occurs at a precursor-polymer concentration well above the overlap threshold; also, the effect of dangling chains can be directly quantified by knowledge of the amount of cross-linker in the linear precursor polymer chains. If in these gels the cross-linking density is homogeneously distributed, the elastic modulus is independent of the length scale of observation. If, in contrast, the cross-linking density exhibits strong spatial fluctuations, the measured elastic modulus decreases when the experimental length scale becomes larger than the length scale of these inhomogeneities. This is because the different nanoscopic gel regions deform in a nonaffine fashion, with the densely cross-linked domains embedded within an easily deformable, less cross-linked background that mostly contributes to the gel elasticity. In addition, the elastic moduli of swollen heterogeneous gels are lower than those of corresponding swollen homogeneous gels, because the swelling is more pronounced for the heterogeneous gels. These findings suggest that when polymeric gels are used in applications such as those as superabsorbent materials[41] or to mimic biological soft tissues,[42] it should be considered that their mechanical properties vary with the size of commonly present polymer-network inhomogeneities compared to the length scale on which these properties are relevant for a given application.

■ ASSOCIATED CONTENT

Supporting Information

Experimental details on the preparation of polymer gel samples and on the AFM measurements. The Supporting Information is available free of charge on the ACS Publications website at DOI: 10.1021/acsmacrolett.5b00228.

■ AUTHOR INFORMATION

Corresponding Author

*E-mail: seiffert@chemie.fu-berlin.de.

DOI: 10.1021/acsmacrolett.5b00228
ACS Macro Lett. 2015, 4, 698−703

Author Contributions

†These authors contributed equally (F.D.L. and J.H.).

Notes

The authors declare no competing financial interest.

■ ACKNOWLEDGMENTS

This work was supported by the collaborative Berlin Joint Lab for Supramolecular Polymer Systems (BerSuPol) between FU Berlin and Helmholtz-Zentrum Berlin and by the Focus Area NanoScale at FU Berlin.

■ REFERENCES

(1) Almdal, K.; Dyre, J.; Hvidt, S.; Kramer, O. *Polym. Gels Networks* **1993**, *1*, 5−17.
(2) Tanaka, T. In *Encyclopedia of Polymer Science and Engineering*; Klingsberg, A., Piccininni, R., Eds.; John Wiley & Sons: New York, 1987; Vol. 7.
(3) Dušek, K.; Prins, W. *Adv. Polym. Sci.* **1969**, *6*, 1−102.
(4) Weiss, N.; Van Vliet, T. T.; Silberberg, A. *J. Polym. Sci., Polym. Phys. Ed.* **1979**, *17*, 2229−2240.
(5) Weiss, N.; Van Vliet, T. T.; Silberberg, A. *J. Polym. Sci., Polym. Phys. Ed.* **1981**, *19*, 1505−1512.
(6) Kizilay, M. Y.; Okay, O. *Polymer* **2003**, *44*, 5239−5250.
(7) Shibayama, M. *Macromol. Chem. Phys.* **1998**, *199*, 1−30.
(8) Horkay, F.; Hecht, A. M.; Geissler, E. *Macromolecules* **1989**, *22*, 3356−3361.
(9) Takata, S.; Norisuye, T.; Shibayama, M. *Macromolecules* **2002**, *35*, 4779−4784.
(10) Nie, J.; Du, B.; Oppermann, W. *Macromolecules* **2004**, *37*, 6558−6564.
(11) Mallam, S.; Shibayama, M. *Bull. Chem. Soc. Jpn.* **2006**, *79*, 1799−1819.
(12) Saalwächter, K. *J. Am. Chem. Soc.* **2003**, *125*, 14684−14685.
(13) Habicht, A.; Schmolke, W.; Lange, F.; Saalwächter, K.; Seiffert, S. *Macromol. Chem. Phys.* **2014**, *215*, 1116−1133.
(14) Aoki, H.; Tanaka, S.; Ito, S.; Yamamoto, M. *Macromolecules* **2000**, *33*, 9650−9656.
(15) Madsen, F. B.; Daugaard, A. E.; Fleury, C.; Hvilsted, S.; Skov, A. L. *RSC Adv.* **2014**, *4*, 6939−6945.
(16) Orakdogen, N.; Okay, O. *Polym. Bull.* **2006**, *57*, 631−641.
(17) Di Lorenzo, F.; Seiffert, S. *Macromol. Chem. Phys.* **2014**, *215*, 2097−2111.
(18) Lindemann, B.; Schröder, U. P.; Oppermann, W. *Macromolecules* **1997**, *30*, 4073−4077.
(19) Seiffert, S.; Oppermann, W.; Saalwächter, K. *Polymer* **2007**, *48*, 5599−5611.
(20) Liu, R.; Oppermann, W. *Macromolecules* **2009**, *42*, 9195−9198.
(21) Grube, S.; Oppermann, W. *Macromolecules* **2013**, *46*, 1948−1955.
(22) Flory, P. J. *Principles of Polymer Chemistry*; Cornell University Press: New York, 1953.
(23) Flory, P. J. *Polym. J.* **1985**, *17*, 1−12.
(24) Chassé, W.; Lang, M.; Sommer, J.; Saalwächter, K. *Macromolecules* **2012**, *45*, 899−912.
(25) Viers, D. B.; Mark, J. E. *J. Macromol. Sci.* **2007**, *44*, 131−138.
(26) Falender, J. R.; Yeh, G. S. Y.; Mark, J. E. *J. Am. Chem. Soc.* **1979**, *101*, 7353−7356.
(27) Rubinstein, M.; Panyukov, S. *Macromolecules* **1997**, *30*, 8036−8044.
(28) Sommer, J.; Lay, S. *Macromolecules* **2002**, *35*, 9832−9843.
(29) Michalke, W.; Lang, M.; Kreitmeier, S.; Göritz, D. *J. Chem. Phys,.* **2002**, *117*, 6300−6307.
(30) Ramzi, A.; Rharbi, Y.; F. Boue, F.; Hakiki, A.; Bastide, J. *Faraday Discuss.* **1995**, *101*, 167−18.
(31) Seiffert, S.; Weitz, D. A. *Soft Matter* **2010**, *6*, 3184−3190.
(32) Beer, F. B.; Johnston, E. R., Jr.; DeWolf, J. T.; Mazurek, D. F. *Mechanics of Materials*; McGraw-Hill: New York, 1981.
(33) Yoon, J.; Cai, S.; Suo, Z.; Hayward, R. C. *Soft Matter* **2010**, *6*, 6004−6012.
(34) Li, C.; Hu, Z.; Li, Y. *Phys. Rev. E* **1993**, *48*, 603−606.
(35) Ahmed, Z.; Gooding, E. A.; Pimenov, K. V.; Wang, L.; Asher, S. A. *J. Phys. Chem. B* **2009**, *113*, 4248−4256.
(36) Flores-Merino, M. V.; Chirasatitsin, S.; LoPresti, C.; Reilly, G. C.; Battaglia, G.; Engler, A. J. *Soft Matter* **2010**, *6*, 4466−4470.
(37) Abidine, Y.; Laurent, V. M.; Michel, R.; Duperray, A.; Palade, L. I.; Verdier, Cl. *Europhys. Lett.* **2015**, *109*, 38003.
(38) Flory, P. J.; Rehner, J., Jr. *J. Chem. Phys.* **1943**, *11*, 512−520.
(39) Erman, B.; Flory, P. J. *Macromolecules* **1986**, *19*, 3242−3253.
(40) Quesada-Perez, M.; Alberto Maroto-Centeno, J.; Forcada, J.; Hidalgo-Alvarez, R. *Soft Matter* **2011**, *7*, 10536−10547.
(41) Buchholz, F. L.; Graham, A. T. *Modern Superabsorbent Polymer Technology*; Wiley VCH: Weinheim, Germany, 2000.
(42) Ping Gong, J. *Science* **2014**, *344*, 161−162.

DOI: 10.1021/acsmacrolett.5b00228
ACS Macro Lett. 2015, 4, 698−703